Dalton Transactions

ROYAL SOCIETY OF CHEMISTRY

PAPER

View Article Online
View Journal | View Issue

Cite this: *Dalton Trans.*, 2025, **54**, 15754

Palladium(II) anticancer agents: the intricate case of the Pd–spermine complex

João A. V. Santos, [a] Maria M. Félix,[a,b] Clara B. Martins,[a,c] Joana Marques, [a] M. Paula M. Marques *[a,c] and Luís A. E. Batista de Carvalho [a]

Palladium-based anticancer drugs are promising alternatives to platinum agents, with potential to overcome acquired resistance and reduce side effects. Among them, the dinuclear Pd(II)–spermine complex (Pd_2Spm) has shown notable cytostatic activity *in vitro*. However, its synthesis mechanism and structural properties remain poorly understood, which hinders further development. This study reports an optimised synthetic route for Pd_2Spm, revealing pH dependence and temperature-induced isomeric changes. These variations were thoroughly characterised by vibrational spectroscopy, leading to the identification of the pure diastereomer (*R*,*S*), the enantiomeric mixture ((*R*,*R*) and (*S*,*S*)) and the mixture containing these three isomers. Cell viability tests were carried out in the human triple negative breast cancer MDA-MB-231 cell line for the diastereomer and the enantiomers and diastereomer mixture, demonstrating equivalent results for these entities (IC_{50} equal to 2.7 and 2.6 μM at 72 h, respectively). This is the first report of an optimised synthesis and anticancer *in vitro* assays for a well-defined Pd_2Spm structure. The present findings strengthen the potential of Pd_2Spm as a next-generation anticancer metallodrug, paving the way for preclinical trials.

Received 31st July 2025,
Accepted 25th September 2025

DOI: 10.1039/d5dt01835h

rsc.li/dalton

1. Introduction

As cancer continues to pose a significant global challenge, the development of new anticancer drugs remains a cornerstone in advancing cancer treatment strategies.[1–3] In 2022 alone, there were 18.74 million cancer diagnoses worldwide (excluding non-melanoma skin cancer), and 9.74 million reported deaths, showing the severe impact of the problem around the world.[4] Although many therapeutic strategies have been explored in recent years, chemotherapy is still one of the most prolific approaches for cancer treatment,[5] both in terms of developing new cytostatic agents and improving the pharmaceutical and physicochemical properties of established anticancer drugs.[6–9]

Building on earlier advances with drugs such as mustin, a pivotal milestone in the evolution of modern chemotherapy was Rosenberg's serendipitous discovery of the antiproliferative properties of cisplatin (*cis*-$Pt(NH_3)_2Cl_2$, cDDP – Fig. 1A),[10] which was the first metal-based anticancer agent, a square-planar complex with a Pt(II) centre coordinated to two ammine ligands and two leaving chloro moieties. Cisplatin has proven to be effective in treating several types of cancer and was approved for pharmaceutical use by the US Food and Drug Administration (FDA) more than 40 years ago.[11] Since then, significant progress has been made in understanding the mechanisms of action of metallodrugs, leading to the development of several compounds containing metal centres such as Pt(II), Pt(IV), Ru(II), Ru(III), Pd(II), Cu(II), Au(I) and Au(III), aiming at an enhanced therapeutic effectiveness and biosafety.[12–14] Targeting capabilities may also be achieved through the combination of these metallodrugs with nanodelivery systems, further improving the anticancer potential of these molecules.[6,15,16]

The advancements on platinum-based cytostatic agents research also led to new families of molecules, such as polynuclear Pt(II)–polyamine complexes, which are particularly interesting due to their unconventional mechanism of action –

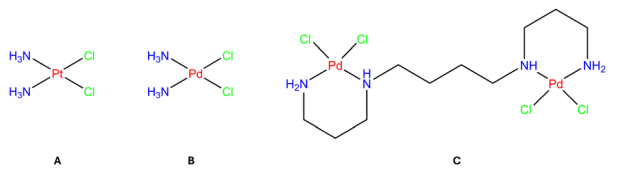

Fig. 1 Pt(II) and Pd(II) complexes with ammines as non-leaving ligands and chloro as leaving groups: (A) *cis*-diamminedichloroplatinum (cDDP); (B) *cis*-diamminedichloropalladium (cDDPd); (C) Pd(II)–spermine complex (Pd_2Spm).

[a]*University of Coimbra, Department of Chemistry, Molecular Physical-Chemistry (QFM-UC), LAQV Requimte, 3004-535 Coimbra, Portugal. E-mail: pmc@ci.uc.pt*
[b]*University of Coimbra, Faculty of Medicine, 3000-548 Coimbra, Portugal*
[c]*University of Coimbra, Department of Life Sciences, 3000-456 Coimbra, Portugal*

yielding interactions with DNA at multiple sites *via* long-range interstrand binding (to the nitrogen atoms from the bases), which trigger a more severe damage to cancer cells as compared to conventional mononuclear Pt(II) compounds such as cDDP.[17,18]

In addition, Pd(II)-drugs have also been widely considered, due to their structural and coordination chemistry similarities to Pt(II)-based agents.[19–22] Moreover, it has been proven that despite the highest lability of Pd(II) complexes (10^5 times higher than their Pt(II) counterparts), they can easily be stabilised by strongly coordinating ligands (*e.g.* N-containing bulky donors) with carefully chosen leaving groups, conferring structural integrity for a long enough period to ensure therapeutic activity.

Interest in palladium-based drugs dates to the early days of anticancer research,[20,23–25] though initial efforts faced setbacks due to the lack of biological activity observed in preliminary cytotoxicity assays comparing cDDP with its analogous form, *cis*-diamminedichloropalladium(II) (cDDPd – Fig. 1B).[26] It was then understood that the lack of activity stemmed from the lability of Pd(II) complexes, much higher when compared with Pt(II).[27] This challenge was later tackled by lowering this kinetic lability through the use of bulky ligands, affording Pd(II) complexes with promising physicochemical and pharmaceutical properties.[28] Spermine, $(H_2N(CH_2)_3NH(CH_2)_4NH(CH_2)_3NH_2$, Spm) was identified in this context as a suitable chelating ligand, leading to the synthesis of a stable complex known as Pd_2Spm (Fig. 1C),[29,30] which has been extensively studied as a cytostatic agent against several types of cancer, such as triple negative breast cancer (TNBC), prostate cancer and osteosarcoma.[13,31–37] Spermine has also been reported as a suitable chelating agent for other types of metal centres, such as Cu(II), further supporting its potential as a promising precursor for metal-based anticancer drugs.[38,39]

Furthermore, the study of Navarro-Ranninger *et al.*[29] perfectly highlights the potential of this cytostatic agent, as compared with the mononuclear Pd(II)–spermine complex (1 : 1 stoichiometry), having shown that Pd_2Spm was significantly more efficient in terms of inherent anticancer activity.

Although being considered a promising candidate as an anticancer agent,[30,40] to the authors' knowledge no research has been carried out to fully understand its synthesis mechanisms and reactivity. The lack of information on how this system evolves during its synthetic process may also hinder Pd_2Spm *in vitro* assays, due to possible unwanted secondary reactions and difficult purification processes that might hamper its application. This way, poor control of this synthetic pathway might be the reason for some variations that have been found in previous studies,[31,41] further justifying the current research, which aims at filling these gaps, using vibrational spectroscopy to clearly characterize Pd_2Spm's synthetic pathway. A thorough understanding of the intricacies of this system led to the identification of three distinct Pd_2Spm forms: the (*R*,*S*)-diastereomer, a (*R*,*R*) and (*S*,*S*) enantiomeric mixture and the ternary mixture containing all of these forms. Biological assays were conducted on the (*R*,*S*) diastereomer and the ternary mixture as representative forms of the complex, enabling a proof-of-concept assessment of anticancer activity in human cancer cells and highlighting Pd_2Spm as a potential alternative to classical metal-based chemotherapeutic agents.

2. Materials and methods

2.1. Reagents and chemicals

Potassium tetrachloropalladate(II) (K_2PdCl_4, 98%), spermine (*N*,*N*′-bis(3-aminopropyl)butane-1,4-diamine, 99%), Dulbecco's Modified Eagle's (high-glucose) cell growth medium (DMEM-HG), phosphate-buffered saline (PBS), sodium bicarbonate ($NaHCO_3$, ≥99.0%), trypan blue (0.4% w/v), trypsin–EDTA (1×) and 3-(4,5-dimethylthiazol-2-yl)-2,5-diphenyltetrazolium bromide (MTT) were purchased from Sigma-Aldrich Química S.L. (Sintra, Portugal). All inorganic salts, acids and bases were also purchased from the same supplier, being carefully selected according to the necessities of high purity and quality. All solvents used in this work were of analytical grade. Fetal bovine (FBS) was acquired from Gibco-Life Technologies (Porto, Portugal).

2.2. Synthesis of Pd_2Spm

In this study, three different Pd_2Spm batches were synthesised, with slight variations in synthesis conditions:

Sample A: Pd_2Spm was prepared following the classical method described in the literature,[30] with few modifications. Briefly, spermine (1.1 mmol–222.4 mg) was dissolved in a minimal amount of water to obtain a clear solution (pH ~ 12). A concentrated aqueous solution of K_2PdCl_4 (2 mmol–652.8 mg) was then added dropwise, under stirring and at a controlled temperature of 20 °C, immediately forming a brownish powder. The suspension was left 2 h under stirring, culminating in the isolation of a brown powder which was filtered, washed with water and ethanol, and left under vacuum overnight. Yield: 64% – 356.5 mg.

Sample B: This batch was prepared following the previously described method, with optimisations to assess the influence of the pH on the reaction. Similarly to sample A, a concentrated solution of spermine (1.1 mmol–222.4 mg) was prepared, with an initial pH of *ca.* 12. This solution was acidified by adding 1 M HCl until the pH reached 4.0. A 2 mmol (652.8 mg) solution of K_2PdCl_4 was then added dropwise. The pH of the homogenised mixture was gradually increased by adding 1 M KOH until a yellowish precipitate formed (at pH equal to 6.78). The mixture was left in a slurry for 24 h at 20 °C, after which the final reaction product was filtered, washed with water and ethanol, and dried under vacuum overnight (sample B1, identified as the mixture of both the (*S*,*S*) and (*R*,*R*) enantiomers and the (*R*,*S*) diastereomer). During reproducibility studies, a precipitate was isolated from the slow evaporation of the mother liquor of this reaction. For simplicity, this distinct Pd_2Spm form was designated as sample

B2, corresponding to (*R*,*S*) diastereomer. Yield: sample B1 – 53% (295.2 mg); sample B2 – 37% (206.1 mg).

Sample C: This batch resulted from the application of the protocol used for sample B, with variations in temperature ranging from 50 to 100 °C. The product obtained was identified as being the enantiomeric (*S*,*S*) and (*R*,*R*) mixture, with a very poor solubility in water. Yield: 50 °C – 79%; 60 °C – 80%; 70 °C – 83%; 80 °C – 66%; 90 °C – 54%; 100 °C – 20%.

Full characterisation of each sample is presented in Tables S1 and S2 (SI – elemental analysis and vibrational spectroscopy (Raman and FTIR), being compared to previously published data[40]). ^{1}H NMR data is presented in Fig. S1, SI – general spectrum since it was not possible to distinguish between Pd_2Spm forms.

2.3. Elemental analysis

Elemental analysis was conducted on a Thermo Finnigan-CE Instruments Flash EA 1112 CHNS series element analyser (Thermo Fisher Scientific, Waltham, MA, USA). Each sample was left under vacuum overnight to guarantee complete dryness, 2–3 mg of the final solid sample being weighted and measured. The data was acquired in duplicate, and the results were only considered if they were in accordance with the replicate of each independent sample.

2.4. Proton nuclear magnetic resonance

Proton Nuclear Magnetic Resonance (^{1}H NMR) spectroscopy was carried out for all reaction products in D_2O solution (18 mM), on a Bruker Avance III 400 NMR spectrometer (400.13 MHz, Bruker, Billerica, USA). The signal of the residual non-deuterated water was taken as a reference (4.79 ppm).

2.5. Vibrational spectroscopy

Fourier transform infrared spectroscopy in attenuated total reflectance mode (FTIR-ATR) was performed (in the mid-infrared region, 400–4000 cm^{-1}) for each synthesised product. The spectra were recorded at room temperature in a Bruker Vertex 70 FTIR spectrometer (Bruker Optik GmbH, Ettlingen, Germany), purged by CO_2-free dry air, using a Bruker Platinum single reflection diamond accessory. The spectrometer was equipped with a liquid nitrogen-cooled wideband mercury cadmium telluride (MCT) detector and a Ge on KBR substrate beamsplitter. The spectra were acquired with a sum of 128 scans at 2 cm^{-1} resolution, and a 3-term Blackman-Harris apodization function was applied. The OPUS 8.1 software was used for data processing: (i) atmospheric compensation (CO_2 and H_2O) and (ii) frequency dependence of the electric field depth in ATR (a mean refractive index of 1.25 was considered).

Raman spectra were measured using a WITec confocal Raman microscope system alpha 300R coupled to an ultra-high-throughput spectrometer (UHTS) 300Vis-NIR (Oxford Instruments WITec, Ulm, Germany). The detection system consisted of a thermoelectrically cooled (−55 °C) charged-coupled device (CCD) front-illuminated camera, with NIR/VIS antireflection coating and 1650 × 200 pixels (spectral resolution <0.8 cm^{-1} per pixel). A 785 nm diode laser was used as exciting radiation (*ca.* 50 mW at the sample position). Each spectrum is the result of 120 accumulations with a 20 s integration time. Cosmic-ray removal was carried out using the WITec Control FIVE 5.1 software (Oxford Instruments WITec, Ulm, Germany).

2.6. Cell culture and biological assays

The human triple-negative breast cancer (TNBC) MDA-MB-231 cell line was purchased from ATCC (Manassas, VA, USA – ATCC HTB 26). The cells were cultured as a monolayer in 75 cm^2 cell culture flasks, in DMEM-HG cell culture medium supplemented with 10% (v/v) inactivated FBS, at 37 °C in a humidified atmosphere with 5% CO_2, and were sub-cultured twice a week (doubling time equal to 25 h).[12]

After verifying a proper cell growth, the cells were harvested upon addition of trypsin–EDTA solution, seeded in 96-well plates at 1.5 × 10^4 cells per cm^2 and left to attach for 24 h. After cell adhesion, different concentrations of Pd_2Spm (0.5 to 90 μM, from a 2 mM stock solution in PBS) were added, except to the cell control group for which only an equivalent amount of culture medium was added. The cells were further incubated for 24, 48 and 72 h previously to the cell viability tests, to enable a viable comparison with previously reported data.[31,40]

After each incubation period, the cell viability was evaluated by the MTT method.[42] Briefly, a MTT solution (0.5 mg mL^{-1} in PBS) was added to each well, followed by 3 h incubation at 37 °C, after which the media was aspirated and DMSO was added to solubilise the formazan crystals formed by reaction with MTT. The optical density at 570 nm was then measured for each sample, to determine half-maximal inhibitory concentration values (IC_{50}) values. These assays were performed to determine the IC_{50} values of samples B1 and B2. Sample C could not be tested, due to its very low water solubility.

2.7. Statistical data analysis

Data from the MTT assays are expressed as the mean ± standard deviation (SD). The GraphPad Prism 7 Software (San Diego, CA, USA) was used, applying the standard one-way ANOVA followed by Dunnett's *post hoc t*-test, for statistical comparison between groups at the same time point. The IC_{50} values were calculated by interpolation from the nonlinear regression curves obtained from the cell viability tests, using "log(inhibitor) *versus* the normalised response-variable slope equation". A *p*-value lower than 0.05 was considered as statistically significant.

3. Results and discussion

3.1. Pd_2Spm synthesis

The first step towards understanding the chemistry of the Pd (II)–spermine complex ($C_{10}H_{26}N_4Cl_4Pd_2$) is to explore what is known so far about its synthesis. As reported by Navarro *et al.*[29] and Codina *et al.*,[30] this would be a simple process in which stoichiometric amounts of a palladium salt (in aqueous solution) are added dropwise to an aqueous solution of sper-

mine. The obtained suspension is then left in a slurry, filtered after 24 h and washed with ethanol, yielding a yellowish powder identified as Pd_2Spm. Despite being seemingly easy to implement, this synthesis is far from straightforward, including undesired secondary products which reveal intricate reaction mechanisms.

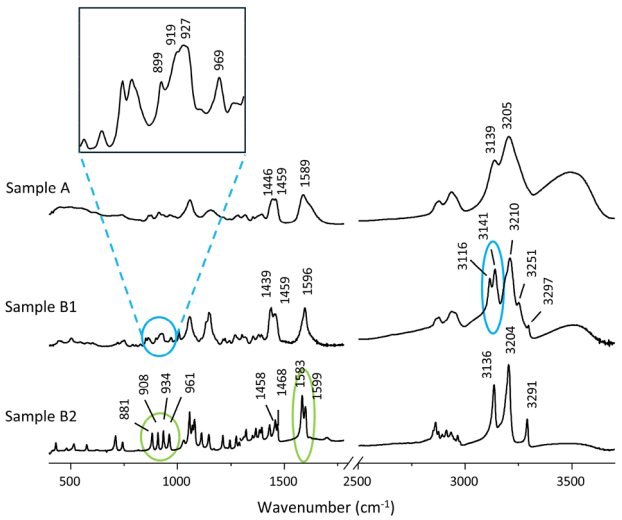

Fig. 2 FTIR-ATR spectra of the reaction products obtained from the different Pd_2Spm synthesis methods: sample A – brownish compound from synthesis without pH control; sample B1 – yellowish powder from optimised synthesis with pH control; sample B2 – yellowish powder precipitated form solution during sample B1 reproducibility tests.

3.1.1. Pd_2Spm synthesis – pH dependence. Spermine is a polyamine with pK_a values between 8 and 12.[43–45] When dissolved in water, an equilibrium will be established, favouring the protonation at each nitrogen atom, particularly the two terminal amine groups. This protonation effectively alters the reactivity of the ligand, leading to different reaction products. To understand this effect, two batches of Pd_2Spm were prepared independently, at a controlled temperature of 20 °C, and different pH values: (i) sample A – Spm was solubilised in water and the pH was determined to be 12.29. No further adjustments were made, and the synthesis was carried out as previously reported, yielding a brownish compound; (ii) sample B – after solubilisation of Spm in water, the pH was lowered to 4.0 ensuring full protonation of the ligand (to Spm^{4+}). Potassium tetrachloropalladate(II) was then added dropwise. To induce complex formation, the deprotonation of Spm^{4+} was controlled through the gradual increase of medium pH by adding a KOH solution, until a yellowish precipitate formed. The powder was left in a slurry for 24 h, isolated and dried as described. The infrared spectra of each of these products (A and B) are depicted in Fig. 2, and the most relevant band assignments are comprised in Table 1.

Table 1 FTIR-ATR and Raman wavenumbers for the Pd_2Spm forms obtained by the optimised synthetic procedures

Literature[a]		Sample A		Sample B1		Sample B2		Sample C		
FTIR	Raman	FTIR	Raman	FTIR	Raman	FTIR	Raman	FTIR	Raman	Assignments
—	—	—	—	3297	—	3291	—	—	—	$\nu_{as}(NH_2)$
3253	3221	—	—	3251	—	—	—	3252	—	$\nu_{as}(NH_2)$
3215	—	3205	—	3210	—	3204	—	3217	—	$\nu(NH)$
3142	3146	3139	—	3141	—	—	—	3143	—	$\nu_{s}(NH_2)$
—	—	—	—	3116	—	3136	—	—	—	$\nu_{s}(NH_2)$
1596	1595	1613	—	1596	—	1599	1597	1597	—	$\delta(NH_2)$
—	—	1589	—	—	—	1583	1585	—	—	$\delta(CH_2)_{Chain}$[b]
1458	1454	1459	—	1459	—	1468	1450	1457	—	$\delta(CH_2)_{Ring}$
1449	1442	1446	—	1439	—	1458	1435	1434	—	$\delta(CH_2)_{Ring}$
—	1147	—	—	—	1148	—	1169	—	1149	ν(C–C)
—	1131	—	—	—	1135	—	1140	—	1134	$\rho(CH_2)_{Chain}$
—	1120	—	—	—	1122	—	—	—	1123	ν(C–C)
1133	1108	—	—	1136	1106	1111	1116	1133	1112	$\omega(NH_2)$
969	—	—	—	969	—	961	—	970	—	ν(C–C)
—	—	—	—	927	—	934	—	927	—	ν(C–C)[b]
918	—	—	—	919	—	—	—	919	—	ν(C–C)
—	903	—	—	—	—	908	913	—	—	$\rho(CH_2)_{Chain}$[b]
899	861	—	—	899	—	881	885	900	—	$\rho(CH_2)_{Ring}$
—	514	—	—	—	—	516	527	517	—	δ(C–N–C)
502	501	—	504	504	506	500	516	503	506	ν_{s}(N–Pd–N)
449	449	—	462	440–450	455	431	466	450	450	ν_{as}(N–Pd–N)
—	324	—	324	—	328	—	320	—	325	ν_{s}(Cl–Pd–Cl)
—	276	—	304	—	279	—	299	—	274	δ(N–Pd–N)
—	256	—	—	—	258	—	255	—	—	γ ring
—	237	—	242	—	242	—	227	—	243	B(C–C–C) “swinging”
—	203	—	—	—	—	—	171	—	—	δ(N–Pd–Cl)
—	164	—	163	—	166	—	162	—	166	$\tau(C–N)_{ring}$
—	152	—	—	—	153	—	—	—	—	$\gamma_2(C–C–C)_{Chain}$
—	127	—	—	—	—	—	121	—	—	$\gamma_4(C–C–C)_{Chain}$

[a] Vibrational modes were assigned according with the available data.[41] [b] Vibrational modes assigned based of theoretical calculations from the same author.

By analysis of the spectra, a clear difference in the attained products is revealed, confirming that pH plays a critical role in the successful synthesis of Pd_2Spm. At first glance, differences in crystallinity can easily be distinguished between the samples formed in A and B, as indicated by a band broadening which has previously been reported for organic and inorganic molecules to be associated with amorphisation.[46,47] In sample A, only some of the main vibrational modes can be seen, namely stretching bands from the amine groups and C–H deformations from Pd_2Spm rings. In contrast, the attained spectra from sample B are well defined and can be easily assigned to Pd_2Spm, since all the vibrational modes are comparable to those reported by theoretical methods literature.[40] Furthermore, sample B experiments led to the formation of two different entities, identified as sample B1 and sample B2, which will be further discussed.

The first thing to be noted is that, despite seemingly being the same compound with different amorphization degrees, elemental analysis reveals variations in composition that can explain the differences in the spectra (Table S1, SI). While previously undetected due to its inherent lower absorptivity, the atomic composition analysis of sample A shows the presence of an additional entity, acting as an impurity that affects the physicochemical characteristics of the sample. This impurity is palladium oxide, present in a $Pd_2Spm:PdO$ stoichiometry of 1 : 0.8, thus accounting for 40% of the solid product. PdO is known to be a dark powder with negligible solubility in water,[48] conferring a darker brownish colour to the reaction product and significantly lowering its solubility.

Considering the relationship between Pd_2Spm purity and the pH value during synthesis, a reaction mechanism can be proposed (Scheme 1): (i) when the polyamine is dissolved in water, an equilibrium is set favouring amine protonation (pK_a values between 8 and 12), naturally increasing the pH of the medium due to H^+ consumption; (ii) when the palladium salt (K_2PdCl_4) is directly added (sample A), the reaction occurs between the metal centre and the active amine groups (which remains reactive due to the established equilibrium, at higher pH), forming the desired product; (iii) this reaction induces a cycle within the mechanism: the metal centre reacts with the amine, disrupting the pH equilibrium and promoting the deprotonation of the solubilised Spm until a new equilibrium is reached (accompanied by medium pH reduction over time); (iv) the final equilibrium is reached at a pH of 7.83, where the concentration of active Spm is reduced and hydroxide ions are still present. At this stage, the percentage of active amine is low enough for the hydroxide ions to compete for coordination to the residual Pd(II) which is still in the form of salt ($PdCl_4^{2-}$) in solution. This eventually leads to the formation of PdO, resulting in the Pd_2Spm/PdO mixture in sample A (highlighted in red due to the presence of the impurity). If, however, the polyamine is initially solubilised in an aqueous solution at a controlled pH of 4, and the palladium salt is carefully added afterwards, no uncontrolled reaction will occur because all amine groups are protonated and no OH^- ions have formed. Upon gradually raising the pH to 12, all spermine amine groups become activated, leading to the formation of pure Pd_2Spm, as stoichiometric conditions between the palladium salt and the polyamine are achieved (sample B1, Scheme 1 (v)).

Interestingly, during reproducibility studies to validate this method, one of the attempts yielded an unexpected yet rather intriguing result. Despite elemental analysis showing the formation of highly pure Pd_2Spm (Table S1, SI), the corresponding infrared spectrum (sample B2 – Fig. 2) revealed a different profile, with the characteristic NH_2 antisymmetric and symmetric stretching vibrational modes showing significant deviations (Table 1), as did other typical Pd_2Spm vibrational modes, such as CH_2 (from the rings) and NH_2 deformations. Furthermore, a substantial increase in crystallinity could be noted, accompanied by a significant change in the amine groups: complex B1 sample has two pairs of antisymmetric/symmetric NH_2 vibrational modes (3297/3116 cm^{-1} and 3251/3141 cm^{-1}, respectively) but in complex B2 there is only one pair visible (3291/3136 cm^{-1}, respectively).

These intriguing findings suggest a complicated system with molecular and structural variations which might be affected by the conditions at which the reaction is carried out. Moreover, these structural variations may play a crucial role on the biological activity of this compound (namely its anticancer potential), particularly due to different forms present in *in vitro*/*in vivo* assays. This issue is paramount and must be addressed in order to ensure a safe and efficient future pharmaceutical application of the complex.

3.1.2. Pd_2Spm synthesis – stereochemistry studies. The chirality of drug molecules has long been of interest for the pharmaceutical industry. Molecular chirality is often defined as a geometric property of a molecule which cannot be superimposed onto is mirrored image, being a key feature of stereoisomers, in turn being defined as molecules that have the same molecular formula and atomic structure but differ in their three-dimensional arrangement.[49] Stereoisomers can be further divided into enantiomers, molecules that exist as mirror images of each other but cannot be superimposed, and diastereomers, being molecules that are not mirror images and generally have different physical and chemical properties.[50]

Many authors highlighted the significance of this property in unveiling the pharmaceutical activity of compounds, demonstrating variations in physical, chemical and bioactivity properties intrinsically related to molecular structure changes stemming from the presence of chiral centres.[51–55] Ibuprofen and Naproxen (Fig. S2 in SI) are two classical examples: the first one is available as a racemic mixture because, although only the *S*-form is pharmaceutically active, the *R*-enantiomer is rapidly converted into the active form;[56,57] and the second being a great example of a drug were only the *S*(+) – enantiomer is therapeutically active, the *R*(+) – enantiomer causing hepatic toxicity and not showing evident signs of pharmacological activity.[58] Similarly, Pd_2Spm also contains chiral centres in its structure (Scheme 1), although no further studies have been conducted to investigate their impact.

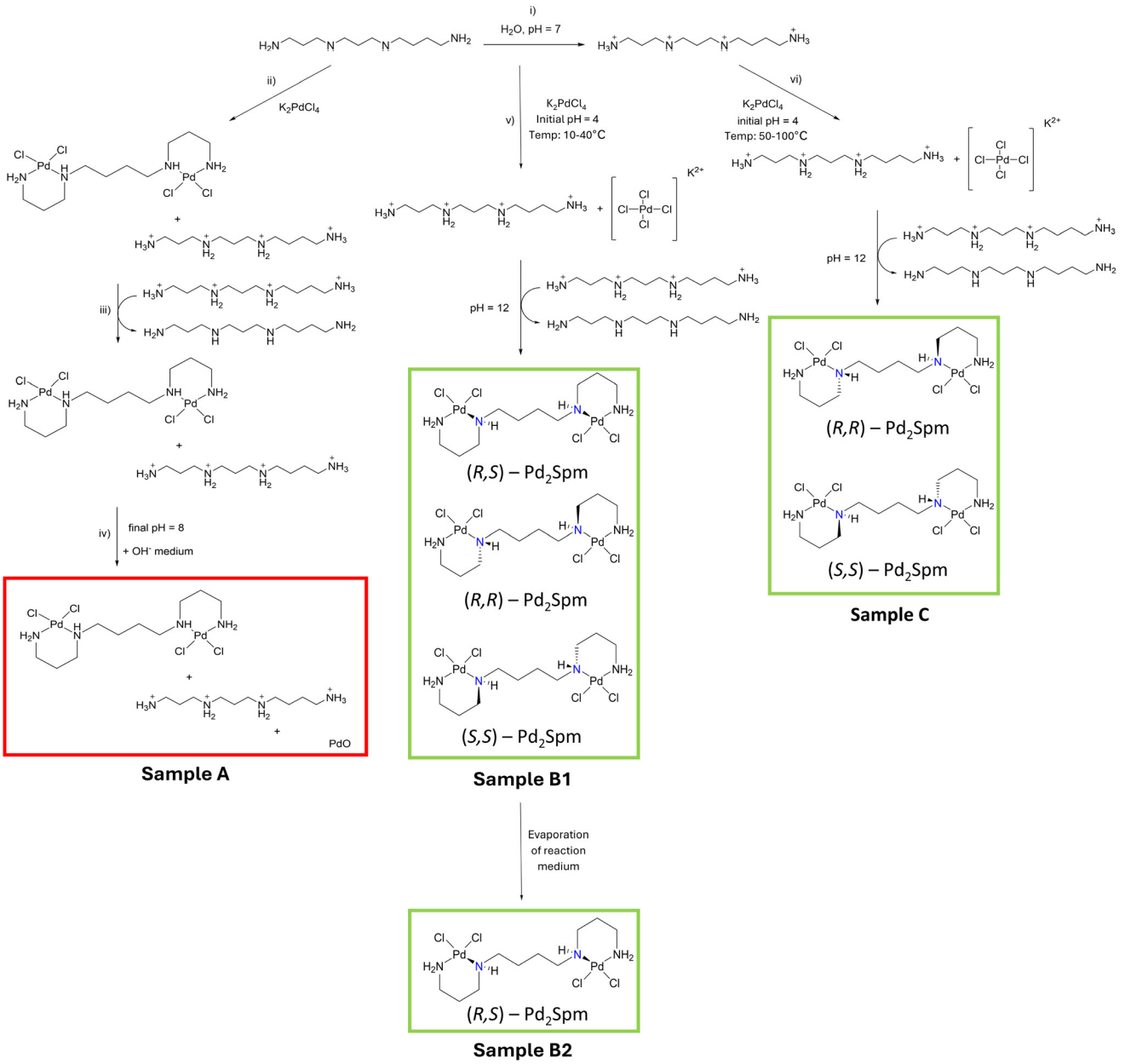

Scheme 1 Proposed mechanism for the synthesis of Pd_2Spm, dependent either on the pH of the medium or the reaction temperature. Final products are highlighted according to purity: sample A is shown in red due to the presence of PdO, whereas samples B1, B2, and C are highlighted in green, indicating pure forms of the Pd(II) complex.

To better understand this baffling relation between chirality and the studied synthetic pathway, a screening process was carried out, implementing the newly optimised synthesis method with controlled pH but at different temperatures, in an attempt to isolate the possible Pd_2Spm conformations: (*R*,*R*), (*S*,*S*) and (*R*,*S*) – forms.

To better understand this baffling relation between chirality and the studied synthetic pathway, a screening process was carried out, implementing the newly optimised synthesis method with controlled pH but at different temperatures, in an attempt to isolate the possible Pd_2Spm conformations: (*R*,*R*), (*S*,*S*) and (*R*,*S*) – forms.

FTIR-ATR spectra were acquired for all the isolated powders, checking for any relations between reaction temperature and the final isomeric form of Pd_2Spm. The most relevant region of the infrared data (2500–3700 cm^{-1}) is presented in Fig. 3 (full spectra in SI – Fig. S3).

Interestingly, the infrared data obtained for the products of the reactions at temperatures ranging from 10 to 100 °C clearly point towards a tendency of Pd_2Spm to stabilise in different forms, depending on the temperature at which the reaction was carried out. This was evidenced by the differences highlighted in the amine stretching region. For a temperature range between 10 and 40 °C, two sets of bands assigned to the

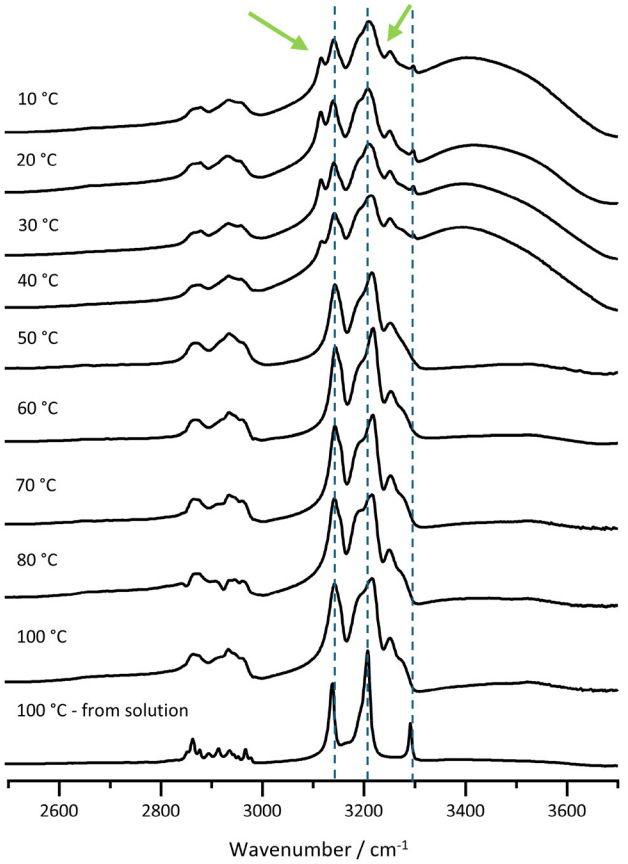

Fig. 3 Infrared spectra of Pd_2Spm powders obtained by reproducing the optimised synthesis method with temperature variation (from 10 to 100 °C). Two groups of equivalent spectra can be observed, according to the temperature range: from 10 to 40 °C and from 50 to 100 °C, showing a clear dependence between the attained product and temperature during the reaction.

antisymmetric/symmetric NH_2 stretching vibrational modes are visible. This profile changes at 50 °C to only one pair of signals (the ones at 3116 and 3297 cm^{-1} disappears). Although with a closer profile to the previously described form obtained in sample B2 (Fig. 2), it is not yet the same, presenting a vibrational mode at around 3252 cm^{-1}, and two other broader bands at 3217 and 3143 cm^{-1}, corresponding to $\nu_{as}(NH_2)$, $\nu(NH)$ and $\nu_s(NH_2)$, respectively.

As it is, it was possible to isolate at least 3 different pure Pd_2Spm samples, each with unique different characteristics. The first, was a crystalline form formerly identified by Codina *et al.*,[30] with a known crystalline structure which revealed to be difficult to reproduce. This form corresponds to the (*R*,*S*) diastereomer of Pd_2Spm (sample B2 in Table 1).

Above 50 °C, a different complex form emerges, which remains stable at the specified temperatures. It has been hypothesised that this form corresponds to the mixture of the (*R*,*R*) and the (*S*,*S*) enantiomers (sample C in Table 1), indistinguishable using FTIR.[59,60] At lower temperatures (between 10 and 40 °C), a mixture of forms is achieved, containing both enantiomers and the diastereomer (sample B1 in Table 1). Since the diastereomer starts forming at temperatures below 40 °C, its presence reveals a shift in reaction product stability with temperature variation, identifying this condition as another key parameter to consider for the synthesis of Pd_2Spm, besides medium pH.

In accordance with the conclusions from pH and temperature variation studies, a direct correlation between the synthesised complexes and the corresponding Pd_2Spm forms can be summarised (Scheme 1): sample A – mixture of Pd_2Spm and PdO; sample B1 – mixture with both enantiomers and the diastereomer of Pd_2Spm; sample B2 – isolated (*R*,*S*) – Pd_2Spm; sample C – mixture of both enantiomers ((*S*,*S*) and (*R*,*R*) – forms), being all referred as the respective forms for this point on.

At this stage, a comprehensive understanding of the Pd_2Spm intricate system has been achieved, revealing it as a palladium based anticancer drug with a synthetic pathway closely dependent on medium pH and reaction temperature.

3.1.3. Pd_2Spm synthesis – Raman spectroscopy insights. To further understand the system from a spectroscopic perspective, Raman spectra were collected for the three described Pd_2Spm forms, being presented in Fig. 4, and the corresponding assignments are comprised in Table 1. The Raman spectrum of the Pd_2Spm–PdO mixture is shown in Fig. S4 (SI), for comparison.

As expected, and in accordance with what was observed in the FTIR-ATR spectra, the spectrum from the (*R*,*S*) – form has a significantly higher crystallinity degree than the other two, leading to well-resolved narrow bands and high signal resolution. On the other hand, both the enantiomeric and the racemic mixture (containing both enantiomers and the diastereomer) present broader signals, associated with a decreased degree of crystallinity.

Due this band broadening effect, a direct comparison between the spectra is challenging. However, clear shifts are observable in several vibrational modes (*e.g.* the bands assigned to ωNH_2, ν_{as}(N–Pd–N) and δ(N–Pd–N), Table 1), rein-

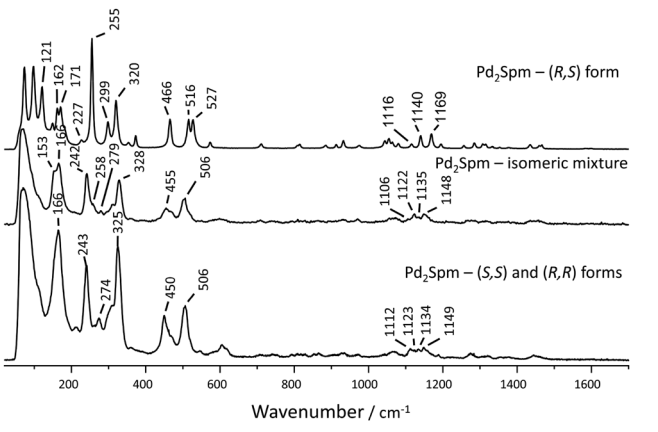

Fig. 4 Raman spectra from the three identified forms of Pd2Spm: the diastereomer (*R*,*S*) – Pd2Spm (complex B2); the enantiomeric mixture of (*R*,*R*) and (*S*,*S*) – Pd2Spm (sample C); the mixture of all the isomers (B1).

forcing the difference between the identified Pd_2Spm species. These three vibrational modes are associated with the amine groups which provide chirality to Pd_2Spm, proving the impact of different Pd_2Spm synthetic protocols on the optical properties of the final complex (*e.g.* role of the pH and temperature as key factors).

3.2. Pd_2Spm – *in vitro* assays in human breast cancer cells

The cytostatic potential of Pd_2Spm has been evaluated through *in vitro* and *in vivo* studies in the last few years,[35,36,61] with reported IC_{50} values between 2.8 and 7.3 μM for the MDA-MB-231 cell line.[31,33,41] This rather broad range of values can be justified by: (i) differences in the protocols used for the *in vitro* assays; (ii) unresolved optical properties of the Pd-complex, due to poorly defined and non-standardized synthetic procedures. In order to address this issue, cell viability assays were presently carried out to determine whether the lower IC_{50} values could be reproduced using the isomeric mixture of the complex. This data is intended to be used as a proof of concept for future pharmacological studies. It should be emphasised that the enantiomeric (*S*,*S*) and (*R*,*R*) mixture was not tested as to its cytotoxic activity since it was found to be poorly soluble in water as opposed to the isomeric mixture containing the enantiomers and the diastereomer.

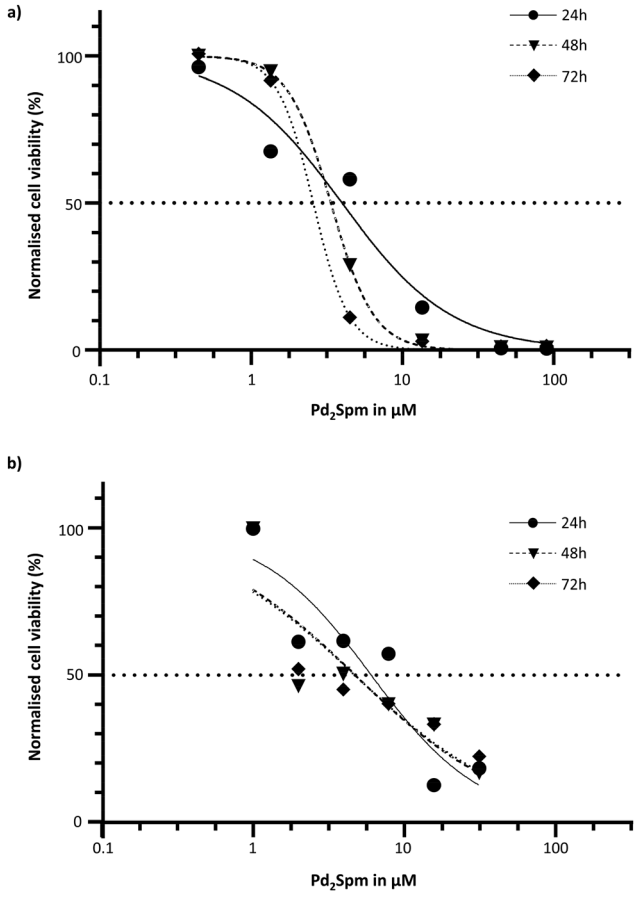

Fig. 5 Graphical representation of cell viability assays carried out for the obtained Pd(II) complexes: (a) the mixture of all isomeric forms; (b) (*R*,*S*) form. Values from one-way ANOVA test. Dunnett's post-test was also used to verify the significance of the obtained results, comparing log IC_{50} means with the control for each time point (the test shows *p*-values <0.0001 for all data points, verifying the significancy of the results).

Table 2 Half maximal inhibitory concentrations (IC_{50}) of Pd2Spm – samples B1 and B2 – against triple negative human breast cancer cells (MDA-MB-231), at 24, 48 and 72 h

Drug	Time	IC_{50} ± SD in μM
Sample B1 – isomeric mixture	24 h	3.99 ± 0.05
	48 h	3.36 ± 0.01
	72 h	2.58 ± 0.01
Sample B2 – (*R*,*S*) form of Pd_2Spm	24 h	5.51 ± 0.11
	48 h	2.41 ± 0.13
	72 h	2.74 ± 0.05

The results presently obtained, shown in Fig. 5 as dose–response curves, revealed a significant decrease in cell viability in the presence of Pd_2Spm, clearly confirming the potential of this molecule as a cytostatic agent, *in vitro*. The nonlinear regression analysis performed to obtain IC_{50} confirmed a half maximal inhibitory concentration of 2.6 μM at 72 h (Table 2), in accordance with the lowest values previously reported.[33,41]

Comparison of the IC_{50} values obtained for the mixture (enantiomers + diastereomer) and the diastereomer of Pd_2Spm (Table 2) evidences that both forms are equivalent in terms of anticancer activity against this type of human cancer cells. These results suggest that the diastereomer (significantly more water soluble) is likely to be the active form. However, there may be advantages in using the isomeric mixture instead of the isolated (*R*,*S*) form, as it is easier to synthesise and may exhibit synergetic activity between the three forms present.

Overall, it is safe to conclude that exposing MDA-MB-231 cells to the (*R*,*S*), (*S*,*S*) and (*R*,*R*) mixture of Pd_2Spm leads to the most promising cytotoxic results reported to this date for this Pd-complex towards this specific type of cancer. A well identified and easily reproducible Pd_2Spm form was currently screened, for the first time. This Pd(II) spermine complex, in this specific mixture (synthesised under mild conditions), is therefore a promising compound to test further in preclinical trials.

4. Conclusions

This study presents the first in-depth evaluation of the chemistry underlying the synthetic pathway to obtain the dinuclear Pd(II)–spermine complex, Pd_2Spm, leading to key findings which are crucial for its development as a potential new anticancer drug: (i) its synthesis is shown to be highly dependent on the reaction conditions (pH and temperature), the pH having been identified as a critical factor for controlling the product's purity and isomeric forms. pH control enabled a deeper understanding of the formation mechanism of Pd_2Spm and the optimisation of the synthetic process (reaction at

room temperature; initial pH of 4, increased to 12 upon addition of the palladium salt); (ii) the known chirality of the complex significantly influences the final product, with the sample's isomeric composition being defined by the temperature of the reaction.

The results from this study evidence that the optimised synthesis protocol at room temperature – pH driven mechanism – yields a mixture of Pd_2Spm isomeric forms – (*S*,*S*) and (*R*,*R*) enantiomers and (*R*,*S*) diastereomer. Furthermore, the data suggest that the latter is the most favoured under these reaction conditions, which may explain the variations observed in previously reported *in vitro* assays, that are probably due to differences in physicochemical properties among Pd_2Spm isomers (leading to distinct biological activities).

Based on these findings, the ternary isomeric mixture was selected for *in vitro* studies and was shown to be the most promising among the several synthesised Pd_2Spm samples (A to C), benefiting from improved water solubility and a similar anticancer potential as the (*R*,*S*) diastereomer. These data are consistent with literature reports on Pd_2Spm as an alternative to classical cytostatic agents such as cisplatin and its derivatives and pave the way for future preclinical trials.

The results obtained in this study contribute to a better understanding of the challenges associated with the synthesis of this dinuclear Pd(II)–polyamine complex and their impact on its biological properties, namely its anticancer activity. Ultimately, this work lays the foundations for further research on Pd_2Spm as a promising candidate for advancing modern chemotherapy.

Author contributions

J. A. V. Santos: Conceptualisation, visualisation, methodology, investigation, formal analysis, writing – original draft preparation. M. M. Félix: Investigation. C. B. Martins: Visualisation, methodology, investigation, formal analysis, and validation. J. Marques: Conceptualization, writing – review & editing, validation, methodology. M. P. M. Marques: Writing – review & editing, validation, resources, methodology, funding acquisition. L. A. E. Batista de Carvalho: Writing – review & editing, validation, resources, methodology, funding acquisition.

Conflicts of interest

There are no conflicts to declare.

Data availability

The data supporting this article have been included as part of the supplementary information (SI). Supplementary information is available. See DOI: **https://doi.org/10.1039/d5dt01835h**.

Acknowledgements

The authors acknowledge the Portuguese Foundation for Science and Technology (FCT) for funding this project, in the scope of the projects UIDB/00070/2020 (**https://doi.org/10.54499/UIDB/00070/2020**) & UIDP/00070/2020 (**https://doi.org/10.54499/UIDP/00070/2020**) and the project UID/50006 – Laboratório Associado para a Química Verde – Tecnologias e Processos Limpos. J. A. V. S., M. M. F. and C. B. M. acknowledge FCT for financial support (PhD grants UIDB/00070/2020, 2024.02780.BD and SFRH/BD/08869/2021). Thanks are due to the UC-NMR facility for recording the NMR spectra.

References

1 D. Sahoo, P. Deb, T. Basu, S. Bardhan, S. Patra and P. K. Sukul, Advancements in platinum-based anticancer drug development: A comprehensive review of strategies, discoveries, and future perspectives, *Bioorg. Med. Chem.*, 2024, **112**, 117894.
2 A. F. Costa, A. Teixeira, C. A. Reis and C. Gomes, Novel anticancer drug discovery efforts targeting glycosylation: the emergence of fluorinated monosaccharides analogs, *Expert Opin. Drug Discovery*, 2025, 193–203.
3 M. Mustafa, M. Rashed and J.-Y. Winum, Novel anticancer drug discovery strategies targeting hypoxia-inducible factors, *Expert Opin. Drug Discovery*, 2025, **20**, 103–121.
4 A. M. Filho, M. Laversanne, J. Ferlay, M. Colombet, M. Piñeros, A. Znaor, D. M. Parkin, I. Soerjomataram and F. Bray, The GLOBOCAN 2022 cancer estimates: Data sources, methods, and a snapshot of the cancer burden worldwide, *Int. J. Cancer*, 2025, **156**, 1336–1346.
5 U. Anand, A. Dey, A. K. S. Chandel, R. Sanyal, A. Mishra, D. K. Pandey, V. De Falco, A. Upadhyay, R. Kandimalla, A. Chaudhary, J. K. Dhanjal, S. Dewanjee, J. Vallamkondu and J. M. Pérez de la Lastra, Cancer chemotherapy and beyond: Current status, drug candidates, associated risks and progress in targeted therapeutics, *Genes Dis.*, 2023, **10**, 1367–1401.
6 J. A. V. Santos, D. Silva, M. P. M. Marques and L. A. E. Batista de Carvalho, Platinum-based chemotherapy: trends in organic nanodelivery systems, *Nanoscale*, 2024, **16**, 14640–14686.
7 M. Yan, S. Wu, Y. Wang, M. Liang, M. Wang, W. Hu, G. Yu, Z. Mao, F. Huang and J. Zhou, Recent Progress of Supramolecular Chemotherapy Based on Host–Guest Interactions, *Adv. Mater.*, 2024, **36**, 2304249.
8 M. S. S. Adam, M. Y. Nassar, M. J. Abdelmageed Abualreish, A. D. M. Mohamad and M. A. Mohamed, Divalent Organo-Bimetallic Chelates of Poly-Dentate O,N,O-dihydrazone Ligand as Effective Agents for Antitumor and Antimicrobial Assays, Interacting Modes With DNA, *Appl. Organomet. Chem.*, 2025, **39**, e7943.
9 J. D. Silva, J. Marques, I. P. Santos, A. L. M. Batista de Carvalho, C. B. Martins, R. C. Laginha, L. A. E. Batista de

Carvalho and M. P. M. Marques, A Non-Conventional Platinum Drug against a Non-Small Cell Lung Cancer Line, *Molecules*, 2023, **28**, 1698.
10 B. Rosenberg, L. Van Camp and T. Krigas, Inhibition of Cell Division in Escherichia coli by Electrolysis Products from a Platinum Electrode, *Nature*, 1965, **205**, 698–699.
11 S. Rottenberg, C. Disler and P. Perego, The rediscovery of platinum-based cancer therapy, *Nat. Rev. Cancer*, 2021, **21**, 37–50.
12 M. Vojtek, C. B. Martins, R. Ramos, S. G. Duarte, I. M. P. L. V. O. Ferreira, A. L. M. Batista de Carvalho, M. P. M. Marques and C. Diniz, Pd(II) and Pt(II) Trinuclear Chelates with Spermidine: Selective Anticancer Activity towards TNBC-Sensitive and -Resistant to Cisplatin, *Pharmaceutics*, 2023, **15**, 1205.
13 T. J. Carneiro, A. L. M. Batista de Carvalho, M. Vojtek, R. C. Laginha, M. P. M. Marques, C. Diniz and A. M. Gil, Pd2Spermine as an Alternative Therapeutics for Cisplatin-Resistant Triple-Negative Breast Cancer, *J. Med. Chem.*, 2024, **67**, 6839–6853.
14 C. M. Andrés, J. M. Pérez de la Lastra, E. Bustamante Munguira, C. A. Juan and E. Pérez-Lebeña, Anticancer Activity of Metallodrugs and Metallizing Host Defense Peptides—Current Developments in Structure-Activity Relationship, *Int. J. Mol. Sci.*, 2024, **25**, 7314.
15 E. Botter, I. Caligiuri, F. Rizzolio, F. Visentin and T. Scattolin, Liposomal Formulations of Metallodrugs for Cancer Therapy, *Int. J. Mol. Sci.*, 2024, **25**, 9337.
16 M. Redrado, Z. Xiao, K. Upitak, B.-T. Doan, C. M. Thomas and G. Gasser, Applications of Biodegradable Polymers in the Encapsulation of Anticancer Metal Complexes, *Adv. Funct. Mater.*, 2024, **34**, 2401950.
17 N. Farrell and Y. Qu, Chemistry of bis(platinum) complexes. Formation of trans derivatives from tetraamine complexes, *Inorg. Chem.*, 1989, **28**, 3416–3420.
18 N. Farrell, in *Platinum-Based Drugs in Cancer Therapy*, ed. L. R. Kelland and N. P. Farrell, Humana Press, Totowa, NJ, 2000, pp. 321–338.
19 M. Vojtek, M. P. M. Marques, I. M. P. L. V. O. Ferreira, H. Mota-Filipe and C. Diniz, Anticancer activity of palladium-based complexes against triple-negative breast cancer, *Drug Discovery Today*, 2019, **24**, 1044–1058.
20 T. J. Carneiro, A. S. Martins, M. P. M. Marques and A. M. Gil, Metabolic Aspects of Palladium(II) Potential Anti-Cancer Drugs, *Front. Oncol.*, 2020, **10**, 590970.
21 T. Scattolin, V. A. Voloshkin, F. Visentin and S. P. Nolan, A critical review of palladium organometallic anticancer agents, *Cell Rep. Phys. Sci.*, 2021, **2**, 100446.
22 K. S. Al-Rashdi, B. A. Babgi, E. M. M. Ali, B. Davaasuren, A.-H. M. Emwas, M. Jaremko, M. G. Humphrey and M. A. Hussien, Dna-binding and antiproliferative properties of Palladium(II) complexes with tridentate ligands, *Inorg. Chim. Acta*, 2024, **561**, 121851.
23 A. Garoufis, S. K. Hadjikakou and N. Hadjiliadis, Palladium coordination compounds as anti-viral, anti-fungal, anti-microbial and anti-tumor agents, *Coord. Chem. Rev.*, 2009, **253**, 1384–1397.
24 M. Fanelli, M. Formica, V. Fusi, L. Giorgi, M. Micheloni and P. Paoli, New trends in platinum and palladium complexes as antineoplastic agents, *Coord. Chem. Rev.*, 2016, **310**, 41–79.
25 R. O. Omondi, S. O. Ojwach and D. Jaganyi, Review of comparative studies of cytotoxic activities of Pt(II), Pd(II), Ru(II)/(III) and Au(III) complexes, their kinetics of ligand substitution reactions and DNA/BSA interactions, *Inorg. Chim. Acta*, 2020, **512**, 119883.
26 J. L. Butour, S. Wimmer, F. Wimmer and P. Castan, Palladium(II) compounds with potential antitumour properties and their platinum analogues: a comparative study of the reaction of some orotic acid derivatives with DNA in vitro, *Chem.-Biol. Interact.*, 1997, **104**, 165–178.
27 B. B. Zmejkovski, N. Đ. Pantelić and G. N. Kaluđerović, Palladium(II) complexes: Structure, development and cytotoxicity from cisplatin analogues to chelating ligands with N stereocenters, *Inorg. Chim. Acta*, 2022, **534**, 120797.
28 J. Hildebrandt, N. Häfner, H. Görls, M.-C. Barth, M. Dürst, I. B. Runnebaum and W. Weigand, Novel Nickel(II), Palladium(II), and Platinum(II) Complexes with O,S Bidendate Cinnamic Acid Ester Derivatives: An In Vitro Cytotoxic Comparison to Ruthenium(II) and Osmium(II) Analogues, *Int. J. Mol. Sci.*, 2022, **23**, 6669.
29 C. Navarro-Ranninger, F. Zamora, J. R. Masaguer, J. M. Pérez, V. M. González and C. Alonso, Palladium(II) compounds of putrescine and spermine. Synthesis, characterization, and DNA-binding and antitumor properties, *J. Inorg. Biochem.*, 1993, **52**, 37–49.
30 G. Codina, A. Caubet, C. López, V. Moreno and E. Molins, Palladium(II) and Platinum(II) Polyamine Complexes: X-Ray Crystal Structures of (SP-4-2)-Chloro{N-[(3-amino-κN) propyl]propane-1,3-diamine-κN,κN′}palladium(1+) Tetrachloropalladate (2−) (2:1) and (R,S)-Tetrachloro[μ-(spermine)]dipalladium(II) (={μ-{N,N′-Bis[(3-amino-κN) propyl]butane-1,4-diamine-κN:κN′}}tetrachlorodipalladium), *Helv. Chim. Acta*, 1999, **82**, 1025–1037.
31 S. M. Fiuza, J. Holy, L. A. E. Batista de Carvalho and M. P. M. Marques, Biologic Activity of a Dinuclear Pd(II)–Spermine Complex Toward Human Breast Cancer, *Chem. Biol. Drug Des.*, 2011, **77**, 477–488.
32 M. P. M. Marques, Platinum and Palladium Polyamine Complexes as Anticancer Agents: The Structural Factor, *Int. Scholarly Res. Not.*, 2013, **2013**, 287353.
33 A. L. M. Batista de Carvalho, P. S. C. Medeiros, F. M. Costa, V. P. Ribeiro, J. B. Sousa, C. Diniz and M. P. M. Marques, Anti-Invasive and Anti-Proliferative Synergism between Docetaxel and a Polynuclear Pd-Spermine Agent, *PLoS One*, 2016, **11**, e0167218.
34 I. Lamego, M. P. M. Marques, I. F. Duarte, A. S. Martins, H. Oliveira and A. M. Gil, Impact of the Pd2Spermine Chelate on Osteosarcoma Metabolism: An NMR Metabolomics Study, *J. Proteome Res.*, 2017, **16**, 1773–1783.
35 T. J. Carneiro, R. Araújo, M. Vojtek, S. Gonçalves-Monteiro, A. L. M. B. de Carvalho, M. P. M. Marques, C. Diniz and A. M. Gil, Impact of the Pd2Spm (Spermine) Complex on

the Metabolism of Triple-Negative Breast Cancer Tumors of a Xenograft Mouse Model, *Int. J. Mol. Sci.*, 2021, **22**, 10775.

36 M. Vojtek, M. P. M. Marques, A. L. M. Batista de Carvalho, H. Mota-Filipe, I. M. P. L. V. O. Ferreira and C. Diniz, Palladium-Spermine Complex (Pd2Spm) Triggers Autophagy and Caspase-Independent Cell Death in Triple-Negative Breast Cancer Cells, *Med. Sci. Forum*, 2022, **14**, 142.

37 R. C. Laginha, C. B. Martins, A. L. C. Brandão, J. Marques, M. P. M. Marques, L. A. E. Batista de Carvalho, I. P. Santos and A. L. M. Batista de Carvalho, Evaluation of the Cytotoxic Effect of Pd2Spm against Prostate Cancer through Vibrational Microspectroscopies, *Int. J. Mol. Sci.*, 2023, **24**, 1888.

38 R. Boggs and J. Donohue, Spermine copper(II) perchlorate, *Acta Crystallogr., Sect. B*, 1975, **31**, 320–322.

39 H. Maluszyńska, A. Perkowska and E. Skrzypczak-Jankun, Crystal and molecular structure of aqua spermine copper (II) sulphate trihydrate studied by X-ray and IR spectroscopy, *J. Chem. Crystallogr.*, 1995, **25**, 19–23.

40 S. M. Fiuza, A. M. Amado, S. F. Parker, M. P. M. Marques and L. A. E. Batista de Carvalho, Conformational insights and vibrational study of a promising anticancer agent: the role of the ligand in Pd(ii)–amine complexes, *New J. Chem.*, 2015, **39**, 6274–6283.

41 M. Vojtek, S. Gonçalves-Monteiro, P. Šeminská, K. Valová, L. Bellón, P. Dias-Pereira, F. Marques, M. P. M. Marques, A. L. M. Batista de Carvalho, H. Mota-Filipe, I. M. P. L. V. O. Ferreira and C. Diniz, Pd2Spermine Complex Shows Cancer Selectivity and Efficacy to Inhibit Growth of Triple-Negative Breast Tumors in Mice, *Biomedicines*, 2022, **10**, 210.

42 T. Mosmann, Rapid colorimetric assay for cellular growth and survival: Application to proliferation and cytotoxicity assays, *J. Immunol. Methods*, 1983, **65**, 55–63.

43 Y. Fukushima and S. Aikawa, Colorimetric detection of spermine and spermidine by zincon in aqueous solution, *Tetrahedron Lett.*, 2019, **60**, 151302.

44 Z. M. Sofian, N. Harun, M. M. Mahat, N. A. N. Hashim and S. A. Jones, Investigating how amine structure influences drug-amine ion-pair formation and uptake via the polyamine transporter in A549 lung cells, *Eur. J. Pharm. Biopharm.*, 2021, **168**, 53–61.

45 G. Rilievo, M. Magro, F. Tonolo, A. Cecconello, L. Rutigliano, A. Cencini, S. Molinari, M. L. Di Paolo, C. Fiorucci, M. N. Rossi, M. Cervelli and F. Vianello, Spermine Oxidase–Substrate Electrostatic Interactions: The Modulation of Enzyme Function by Neighboring Colloidal γ-Fe2O3, *Biomolecules*, 2023, **13**, 1800.

46 A. M. Kaushal, A. K. Chakraborti and A. K. Bansal, FTIR Studies on Differential Intermolecular Association in Crystalline and Amorphous States of Structurally Related Non-Steroidal Anti-Inflammatory Drugs, *Mol. Pharm.*, 2008, **5**, 937–945.

47 J. Dahiya, P. Phogat, A. Hooda and S. Khasa, Investigations of Praseodymium doped LiF-ZnO-Bi2O3-B2O3 glass matrix for photonic applications, *AIP Conf. Proc.*, 2024, **2995**, 020065.

48 M. Muniz-Miranda, A. Zoppi, F. Muniz-Miranda and N. Calisi, Palladium Oxide Nanoparticles: Preparation, Characterization and Catalytic Activity Evaluation, *Coatings*, 2020, **10**, 207.

49 P. Peluso and B. Chankvetadze, Recognition in the Domain of Molecular Chirality: From Noncovalent Interactions to Separation of Enantiomers, *Chem. Rev.*, 2022, **122**, 13235–13400.

50 A. G. Hutt and J. O'Grady, Drug chirality: a consideration of the significance of the stereochemistry of antimicrobial agents, *J. Antimicrob. Chemother.*, 1996, **37**, 7–32.

51 H.-J. Federsel, Facing chirality in the 21st century: Approaching the challenges in the pharmaceutical industry, *Chirality*, 2003, **15**, S128–S142.

52 B. Kasprzyk-Hordern, Pharmacologically active compounds in the environment and their chirality, *Chem. Soc. Rev.*, 2010, **39**, 4466–4503.

53 J. Ceramella, D. Iacopetta, A. Franchini, M. De Luca, C. Saturnino, I. Andreu, M. S. Sinicropi and A. Catalano, A Look at the Importance of Chirality in Drug Activity: Some Significative Examples, *Appl. Sci.*, 2022, **12**, 10909.

54 J. S. Kandula, V. V. S. P. K. Rayala and R. Pullapanthula, Chirality: An inescapable concept for the pharmaceutical, bio-pharmaceutical, food, and cosmetic industries, *Sep. Sci. plus*, 2023, **6**, 2200131.

55 R. U. McVicker and N. M. O'Boyle, Chirality of New Drug Approvals (2013–2022): Trends and Perspectives, *J. Med. Chem.*, 2024, **67**, 2305–2320.

56 V. N. Emel'yanenko, K. V. Zherikova and S. P. Verevkin, Quantum Chemistry and Pharmacy: Diagnostic Check of the Thermochemistry of Ibuprofen, *ChemPhysChem*, 2024, **25**, e202400066.

57 B. S. Ready and P. K. Dubey, Regulatory and Patenting Aspects of Chiral Drugs, *Resonance*, 2024, **29**, 557–571.

58 B. Petrie and D. Camacho-Muñoz, Analysis, fate and toxicity of chiral non-steroidal anti-inflammatory drugs in wastewaters and the environment: a review, *Environ. Chem. Lett.*, 2021, **19**, 43–75.

59 N. Borho, T. Häber and M. A. Suhm, Chiral self-recognition in the gas phase: the case of glycidol dimers, *Phys. Chem. Chem. Phys.*, 2001, **3**, 1945–1948.

60 R.-X. Liang, Q.-Y. Ma, T.-X. Xiang, Y.-P. Zhang, Y.-N. Gong, B. Huang, B.-J. Wang, S.-M. Xie, J.-H. Zhang and L.-M. Yuan, A novel pillar[3]trianglimine macrocycle with a deep cavity used as a chiral selector to prepare a chiral stationary phase by thiol-ene click reaction for enantioseparation in high-performance liquid chromatography, *J. Sep. Sci.*, 2023, **46**, 2300376.

61 M. Vojtek, S. Gonçalves-Monteiro, E. Pinto, S. Kalivodová, A. Almeida, M. P. M. Marques, A. L. M. Batista de Carvalho, C. B. Martins, H. Mota-Filipe, I. M. P. L. V. O. Ferreira and C. Diniz, Preclinical Pharmacokinetics and Biodistribution of Anticancer Dinuclear Palladium(II)-Spermine Complex (Pd2Spm) in Mice, *Pharmaceuticals*, 2021, **14**, 173.

